Contribution from the Department of Chemistry,
University of Minnesota, Minneapolis, Minnesota 55455

Steric Control in the Synthesis and Stereochemistry of the Asymmetric "Head-to-Head" Isomer of Binuclear $[Rh_2(\mu\text{-HTP5})_2(\mu\text{-dppm})_2](PF_6)_2$ (HTP5 = 1,5-Diisocyano-1,1,5-triphenylpentane; dppm = Bis(diphenylphosphino)methane)

Charles A. Daws, Michael G. Hill, John P. Bullock, and Kent R. Mann*

Received November 13, 1990

The reaction of the asymmetrical diisocyanide ligand 1,5-diisocyano-1,1,5-triphenylpentane (HTP5) with $[Rh(dppm)(CO)Cl]_2$ (dppm = bis(diphenylphosphino)methane) results in the exclusive formation of the "head-to-head" *RR* and *SS* isomers of the face-to-face binuclear complex $[Rh_2(\mu\text{-HTP5})_2(\mu\text{-dppm})_2](PF_6)_2$. Herein we report the synthesis and characterization of this complex by ^{31}P NMR, homonuclear 2D δ/J resolved ^{31}P NMR, infrared, and electronic spectra, cyclic voltammetry, and X-ray crystallography. The complex $C_{100}H_{88}F_{12}N_4P_6Rh_2$ crystallizes in the monoclinic space group $C2/c$ with a = 28.74 (1) Å, b = 19.126 (9) Å, c = 21.91 (1) Å, β = 119.74 (4)°, V = 10455 (1) Å^3, and Z = 4. The crystal structure and ^{31}P NMR spectra indicate that only the head-to-head *RR* and *SS* isomers exist in both the solid state and solution. Steric interactions among the pendant phenyl rings direct the dication formation reaction to produce exclusively the head-to-head *RR* and *SS* isomers. These steric interactions also result in different rotameric conformations of the Rh–P bonds at the two Rh centers. The differences in the phenyl ring orientations produce different Rh–P bond lengths, ^{31}P chemical shifts, and ν(CN) stretching frequencies for the "head" and "tail" ends of the molecule. These results contrast with the less hindered compound $[Rh_2(\mu\text{-dimen})_2(\mu\text{-dppm})_2](PF_6)_2$ (dimen = 1,8-diisocyano-*p*-menthane) in which both the "head-to-head" and the "head-to-tail" isomers exist in a 1:1 ratio, and the spectroscopically observable differences in the two ends are less. Further, the radical formed by one-electron oxidation of $[Rh_2(HTP5)_2(dppm)_2](PF_6)_2$ is studied by EPR and UV-vis-IR spectroelectrochemistry.

Introduction

In 1977 it was reported that visible light photolysis of the tetranuclear rhodium complex $[Rh_2(bridge)_4]_2^{6+}$ (bridge = 1,3-diisocyanopropane) in 12 M HCl results in a two-electron oxidative cleavage of the metal complex to $[Rh_2(bridge)_4Cl_2]^{2+}$, with the concomitant reduction of protons to hydrogen gas.[1] Flash photolysis studies of the tetranuclear species in sulfuric acid solutions indicated that the excited-state cleavage of the central Rh–Rh interaction to yield highly reactive $[Rh_2(bridge)_4]^{3+}$ d^7–d^8 radicals occurred in the primary photolytic step.[2] Toward understanding the role of the d^7–d^8 radical in this reaction and the general thermodynamic and kinetic properties required of a system to undergo net multielectron-transfer reactions, we have set out to generate and study binuclear d^7–d^8 radicals.[3-6]

Ongoing studies[6] in this laboratory indicate that the conformation of the bridging ligands affects the thermodynamics of electron-transfer reactions. In an attempt to prepare a binuclear Rh compound that was sterically hindered at the axial sites, $[Rh(dppm)(CO)Cl]_2$ was reacted with 2 equiv of TP5[7] (where dppm = bis(diphenylphosphino)methane; TP5 = 1,5-diisocyano-1,1,5,5-tetraphenylpentane). This uncharacteristically slow reaction did not give the desired $[Rh_2(TP5)_2(dppm)_2]^{2+}$ complex, but gave as the major product $[Rh_2(TP5)_4]^{2+}$. An analogous reaction with the less hindered HTP5 ligand (HTP5 = 1,5-diisocyano-1,1,5-triphenylpentane) in which one phenyl group is replaced by a hydrogen produced the desired $[Rh_2(HTP5)_2(dppm)_2](PF_6)_2$ complex.

As with a previously reported[3,8,9] unsymmetrical diisocyanide ligand, dimen (1,8-diisocyano-*p*-menthane), we expected the use of HTP5 would lead to both "head-to-head" and "head-to-tail" isomers. X-ray studies[3,8,9] and homonuclear 2D δ/J resolved ^{31}P NMR[8] of binuclear complexes containing dimen showed that statistical mixtures of all configurational isomers were obtained.

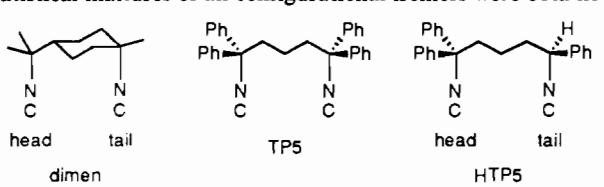

As shown above, the HTP5 ligand has a chiral center at the tail end. Taking into account the chirality of the HTP5 ligand, a total of six different isomers of $[Rh_2(HTP5)_2(dppm)_2](PF_6)_2$ are possible (vide infra). We were therefore surprised to find that of these six isomers only the enantiomeric pair of head-to-head *RR* and *SS* isomers were formed (i.e., both HTP5 ligands in a given molecule have the same chirality). Apparently, replacement of dimen with HTP5 sufficiently increases the energy differences between the configurational isomers to allow the selective formation of a single enantiomeric pair of isomers.

In this paper, we present crystallographic and spectroscopic evidence that the sterically hindered head-to-head *RR* and *SS* isomers of $[Rh_2(HTP5)_2(dppm)_2](PF_6)_2$ are the unique products of the reaction of HTP5 with $[Rh(dppm)(CO)Cl]_2$.

Experimental Section

Synthesis of $[Rh_2(dimen)_2(dppm)_2](PF_6)_2$ Compounds. The starting materials $[Rh(CO)(Cl)(dppm)]_2$,[10] $[Rh_2(dimen)_2(dppm)_2](PF_6)_2$,[3] HTP5,[7] TP5,[7] and dimen[11] were prepared by literature procedures.

$[Rh_2(\mu\text{-HTP5})_2(dppm)_2](PF_6)_2$. $[Rh_2(HTP5)_2(dppm)_2](PF_6)_2$ was synthesized via a modification of the procedure used for $[Rh_2(dimen)_2(dppm)_2](PF_6)_2$. Under a nitrogen atmosphere, 0.133 g (0.381 mmol) of HTP5 in 30 mL of methanol was added dropwise to a slurry of 0.211 g (0.190 mmol) of $[Rh(CO)Cl(dppm)]_2$ in 20 mL of methanol. Addition of 0.0787 g (0.483 mmol) of NH_4PF_6 dissolved in 10 mL of methanol yielded a dark blue precipitate. After the solution was stirred for 40 min, the solid was collected on a fine frit and washed with 1:1 ether/hexanes. The solid was recrystallized from acetone and hexane and dried under vacuum to yield 0.245 g (0.125 mmol) of $[Rh_2(HTP5)_2(dppm)_2](PF_6)$ (66% yield). The fast-atom-bombardment mass spectrum (FABMS) contained a peak pattern at m/e 1820.5 that matched the isotopic distribution calculated for $[Rh_2(HTP5)_2(dppm)_2](PF_6)^+$. IR (Nujol mull): ν(CN) = 2144 s, 2104 s cm^{-1}. IR (CH_2Cl_2): ν(CN) = 2144 s, 2110 s

* To whom correspondence should be addressed.

(1) Mann, K. R.; Lewis, N. S.; Miskowski, V. M.; Erwin, D. K.; Hammond, G. S.; Gray, H. B. *J. Am. Chem. Soc.* **1977**, *99*, 5525.
(2) Miskowski, V. M.; Mann, K. R.; Gray, H. B.; Milder, S. J.; Hammond, G. S.; Ryason, P. R. *J. Am. Chem. Soc.* **1979**, *101*, 4383.
(3) Boyd, D. C.; Matsch, P. A.; Mixa, M. M.; Mann, K. R. *Inorg. Chem.* **1986**, *25*, 3331 and references therein.
(4) Boyd, D. C.; Szalapski, R.; Mann, K. R. *Organometallics* **1989**, *8*, 790.
(5) Boyd, D. C.; Rodman, G. S.; Mann, K. R. *J. Am. Chem. Soc.* **1986**, *108*, 1779.
(6) Hill, M. G.; Mann, K. R. *Inorg. Chem.* **1991**, *30*, 1429.
(7) Hill, M. G.; Comstock, M. C.; Mann, K. R. *J. Org. Chem.* **1990**, *55*, 4950.
(8) Sykes, A. G.; Mann, K. R. *J. Am. Chem. Soc.* **1990**, *112*, 7247.
(9) Mann, K. R. *Cryst. Struct. Commun.* **1981**, *10*, 451.
(10) Mague, J. T.; Mitchener, J. P. *Inorg. Chem.* **1969**, *8*, 119.
(11) Weber, W. P.; Gokel, G. W.; Ugi, I. K. *Angew. Chem., Int. Ed. Engl.* **1972**, *11*, 530.

0020-1669/92/1331-2948$03.00/0

cm^{-1}. ^{31}P NMR (CD_2Cl_2): δ 14.74 (second-order multiplet), 31.74 (second-order multiplet). ^{31}P NMR (acetone) δ 16.84 (second-order multiplet), 32.99 (second-order multiplet). UV–vis (CH_3CN): λ_{max} = 322, 591 nm. Emission (CH_3CN, λ_{ex} = 585 nm): λ_{max} = 676 nm. Anal. Calcd for $C_{100}H_{88}F_{12}N_4P_6Rh_2$: C, 61.11; H, 4.51; N, 2.85; P, 9.46. Found: C, 60.86; H, 4.67; N, 3.12; P, 9.41.

Instrumental Techniques. IR spectra were recorded on a Perkin-Elmer 1710 FTIR. Room temperature UV–vis spectra were recorded on either a Cary 17D spectrometer interfaced to a Zenith 150 microcomputer or a Tracor Northern TN-6500 rapid scan diode-array spectrometer. Solvent background subtraction and plotting of the Cary data were performed with Lotus-123 software. Emission spectra were recorded with a Spec 112X spectrofluorometer operated in ratio mode, and corrected for detector response.

^{31}P and homonuclear 2D δ/J resolved ^{31}P NMR were obtained on either a Varian Unity 300 or a Nicollet NT-300W-B instrument at 121.5 MHz. Chemical shifts for ^{31}P NMR are reported in units of δ, referenced to 85% phosphoric acid as an external standard. All ^{31}P and ^{31}P 2D δ/J NMR spectra are proton decoupled. NMR spectra were simulated on a Zenith 150 microcomputer using the program RACCOON.[12]

X-Band EPR spectra were recorded on a Bruker Model ESP 300 spectrometer equipped with a Bruker ER-4111-VT nitrogen-flow temperature controller. The magnetic field was calibrated with the 2,2-diphenyl-1-picrylhydrazyl hydrate free radical (DPPH) as an external standard (g = 2.0037).[13]

Fast-atom-bombardment mass spectra were obtained on a VG Analytical VG 7070E-HF high-resolution double-focusing mass spectrometer equipped with a VG 11/250 data system. Spectra were obtained at a resolution of 1 part in 2000. Ions were generated by bombardment of the target matrix with a neutral xenon atom beam (derived from a Xe^+ ion beam accelerated at 8 kV). Samples for FABMS were prepared by dissolving the complex in a *m*-nitrobenzoic acid matrix.

Elemental analyses were performed by M-H-W Laboratories of Phoenix, AZ.

Collection and Reduction of Crystallographic Data. Crystals of $[Rh_2(HTP5)_2(dppm)_2](PF_6)_2$ were obtained by forming layers of hexane and diethyl ether over a concentrated solution of the compound in acetonitrile. Crystallization occurred over a period of several days at ambient temperature. To prevent possible loss of solvent from the lattice, a blue rectangular prism of approximate dimensions 0.50 × 0.30 × 0.25 mm was coated with a viscous high-molecular-weight hydrocarbon before it was secured on a glass fiber by cooling to −87 °C.

The automatic peak searching, centering, and indexing routines available on the Enraf-Nonius SDP-CAD4 automatic diffractometer[14] were used to find and center the 25 reflections with $25.6 < 2\theta < 53.0°$ which were used to define the unit cell parameters. Space group assignments were made by examining the data collected for systematic absences and confirmed by the successful solution and refinement of the structure.[15] A total of 7316 reflections was collected using the ω scan technique to a maximum 2θ value of 51.9°. Data were collected in the hkl and $\bar{h}kl$ octants. The intensities of three representative reflections which were measured every 100 min of X-ray exposure time declined by 4.60%. A linear correction factor was applied to the data to account for this phenomena. The structure was solved by direct methods.[16,17] Corrections for Lorentz and polarization effects were made. Using the program DIFABS,[18] an empirical absorption correction was applied. Corrections for extinction were negligible.

Table I. Crystallographic Data and Collection Parameters for $[Rh_2(HTP5)_2(dppm)_2](PF_6)_2$

chem formula	$C_{100}H_{88}F_{12}N_4P_6Rh_2$
a, Å	28.74 (1)
b, Å	19.126 (9)
c, Å	21.91 (1)
β, deg	119.75 (4)
V, Å^3	10455
Z	4
fw	1965.44
space group	$C2/c$ (No. 15)
T, °C	−87
λ, Å	0.710 69 (graphite monochromated)
ρ_{calc}, g cm^{-3}	1.248
μ(Mo Kα), cm^{-1}	8.42
transm factors	0.84–1.25
R	0.127
R_w	0.172

The P, Rh, Br, and F atoms were refined anisotropically; all other non-hydrogen atoms were refined isotropically. The H atom positions were calculated, and the isotropic temperature factor for each H atom was assigned a value 20% larger than B for the atom to which it is attached. The final cycle of full-matrix least-squares refinement was based on 4713 observed reflections and 216 variable parameters. Scattering factors were from Cromer and Waber[19] and included the effects of anomalous dispersion.[20,21] All calculations were performed using the TEXSAN crystallographic software package.[14] Summaries of the crystal data and collection parameters for the complexes are found in Table I.

Table II contains final positional parameters of non-hydrogen atoms in the $[Rh_2(HTP5)_2(dppm)_2]^{2+}$ cation. Selected bond lengths and bond angles are given in Table III. Complete tables of crystal data, positional parameters, bond lengths, bond angles, thermal parameters, a summary of the least-squares planes, and the calculated and observed structure factors are included as supplementary material.

^{31}P and Homonuclear 2D δ/J Resolved ^{31}P NMR. FIDs were collected with a pulse sequence $90°-\tau_1-180°-\tau_1-\text{echo}(t_2)$,[22] with the evolution time t_1 considered as $2\tau_1$ (i.e., the time between the onset of the 90° pulse and the acquisition) ranging incrementally from 5 to 640 ms, and t_2 as the elapsed time of recording the FID. Fourier transformation in both time domains gives a 2D spectrum with two frequency dimensions, f_1 and f_2. Fourier transformation with respect to f_2 gives chemical shift and coupling information. Because t_1 causes modulation in the FID due to P–P coupling constants, f_1 yields values of coupling constants only, with the splitting pattern centered at zero. A 45° "tilting" of the f_2 axis subtracts the P–P coupling contributions. Thus, after tilting, the 2D series of spectra represent a plot of ^{31}P $\{^1H, ^{31}P\text{–}^{31}P\}$ decoupled chemical shifts (f_2) vs P–P couplings (f_1).

Electrochemical Measurements. All electrochemical experiments were performed with a BAS 100 electrochemical analyzer.

Cyclic voltammetry (CV) was performed at ambient temperature (25 °C) with a normal three-electrode configuration consisting of a highly polished glassy-carbon-disk working electrode (A = 0.07 cm^2), and a AgCl/Ag reference electrode containing 1.0 M KCl. The working com-

(12) Schatz, P. F. University of Wisconsin, Project SERAPHIM, 1984. RACCOON was written for the IBM microcomputer.
(13) Drago, R. S. *Physical Methods in Inorganic Chemistry*; W. B. Saunders Co.: Philadelphia, 1977; p 324.
(14) All calculations were carried out with the TEXSAN-TEXRAY Structure Analysis Package, Molecular Structure Corp., 1985.
(15) A complete quadrant was collected from 0° to 18°, but during the collection of the 18–26° data there was a failure in the cooling system and only about half of this quadrant was collected. It was decided to use these data rather than try to collect a new set. The missing data would lower the accuracy of the determination but would not affect R. The space group determination was ambiguous. The $h0l$ reflections with l odd are weak; $I/\sigma(I)$ averages 4.1 for l being odd while it averages 12.2 for l being even. The $N(Z)$ test values fall between centric and acentric which usually suggests the acentric space group. On the other hand, the Patterson appears to fit $C2/c$. The cation and a PF_6^- were located. The latter had too much electron density to be a P atom. As it was possible that Br^- was carried over as an impurity from the HTP5 ligand synthesis, the PF_6^- was treated as a mixture of PF_6^- and Br^-, as is reported. The final occupancy factors are 0.37 for Br^- and 0.63 for PF_6^-. The space group $C2$ was considered by putting Br^- at one position and PF_6^- at the other related by the pseudo-c-glide and then locating the cations one at a time. The cations are identical within experimental error. The largest peaks in the difference map are near the Br^- and PF_6^-. The R values are virtually identical with the values from the $C2/c$ refinement. The temperature factors on the c-glide related atoms are highly correlated. Thus, it is concluded that the space group is really $C2/c$. There is little doubt about the structure of the cation. It has a 2-fold axis, coincident with the Rh–Rh bond, with staggered bonds about the two Rh's as viewed down the axis. It is still uncertain why the R value is so high.
(16) MITHRIL—an integrated direct methods computer program: Gilmore, C. J. *J. Appl. Crystallogr.* **1984**, *17*, 42.
(17) DIRDIF—an automatic procedure for phase extension and refinement of difference structure factors: Beurskens, P. T. Technical Report 1984/1; Crystallography Laboratory, Toernooiveld, 6525 Ed. Nijmegen, The Netherlands.
(18) Walker; Stuart. *Acta Crystallogr.* **1983**, *A39*, 158.
(19) Cromer, D. T.; Waber, J. T. *International Tables for X-ray Crystallography*; The Kynoch Press: Birmingham, England, 1974; Vol. IV, Table 2.2 A.
(20) (a) Ibers, J. A.; Hamilton, W. C. *Acta Crystallogr.* **1964**, *17*, 781. (b) Cromer, D. T. *International Tables for X-ray Crystallography*; The Kynoch Press: Birmingham, England, 1974; Vol. IV, Table 2.3.1.
(21) The function minimized was $w(|F_o| - |F_c|)^2$ where $w = 4F_o^2/\sigma^2(F_o^2)$. The unweighted and weighted residuals are defined in the usual way: The intensity data were processed as described previously.
(22) (a) Aue, W. P.; Karhan, J.; Ernst, R. R. *J. Chem. Phys.* **1976**, *64*, 4266. (b) Aue, W. P.; Bartholdi, E.; Ernst, R. R. *J. Chem. Phys.* **1976**, *64*, 2229.

Table II. Positional Parameters and Equivalent Isotopic Displacement Parameters (Å^2) for the $[Rh_2(HTP5)_2(dppm)_2]^{2+}$ Cation and Their Estimated Standard Deviations

atom	*x*	*y*	*z*	*B*
Rh1	0	0.1388 (1)	1/4	2.1 (1)
Rh2	0	0.2993 (1)	1/4	1.9 (1)
P1	−0.0375 (2)	0.1385 (3)	0.1287 (3)	2.1 (2)
P2	−0.0674 (2)	0.2971 (3)	0.1359 (2)	2.2 (2)
C1P	−0.0568 (7)	0.227 (1)	0.089 (1)	2.4 (4)
C1	−0.0724 (7)	0.134 (1)	0.236 (1)	2.8 (4)
N1	−0.1148 (5)	0.1275 (8)	0.2285 (7)	1.9 (3)
C2	−0.1696 (6)	0.121 (1)	0.2188 (8)	1.6 (3)
C3	−0.1679 (7)	0.134 (1)	0.289 (1)	2.3 (4)
C4	−0.1359 (7)	0.195 (1)	0.329 (1)	2.8 (4)
C5	−0.1599 (7)	0.265 (1)	0.295 (1)	2.7 (4)
C6	−0.1202 (7)	0.330 (1)	0.3255 (9)	1.9 (3)
N7	−0.0786 (5)	0.3171 (9)	0.3076 (7)	2.0 (3)
C7	−0.0503 (7)	0.309 (1)	0.285 (1)	2.4 (4)
C1A	−0.0954 (5)	0.0840 (7)	0.0750 (6)	2.2 (4)
C2A	−0.1243 (5)	0.0954 (7)	0.0026 (7)	4.0 (5)
C3A	−0.1671 (5)	0.0516 (9)	−0.0402 (5)	4.8 (6)
C4A	−0.1809 (5)	−0.0035 (8)	−0.0106 (8)	5.4 (6)
C5A	−0.1519 (7)	−0.0149 (8)	0.0618 (9)	6.9 (7)
C6A	−0.1092 (6)	0.0289 (8)	0.1046 (6)	5.3 (6)
C1B	0.0037 (4)	0.1062 (7)	0.0910 (6)	2.3 (4)
C2B	0.0063 (5)	0.1406 (6)	0.0366 (6)	2.9 (4)
C3B	0.0362 (5)	0.1121 (7)	0.0084 (6)	3.7 (5)
C4B	0.0636 (5)	0.0492 (7)	0.0346 (7)	3.5 (5)
C5B	0.0610 (5)	0.0148 (6)	0.0890 (7)	4.2 (5)
C6B	0.0310 (5)	0.0433 (7)	0.1172 (6)	3.0 (4)
C1C	−0.1354 (3)	0.2902 (7)	0.1176 (6)	2.6 (4)
C2C	−0.1674 (5)	0.2307 (6)	0.0918 (6)	2.6 (4)
C3C	−0.2203 (4)	0.2322 (6)	0.0778 (6)	2.8 (4)
C4C	−0.2412 (4)	0.2933 (7)	0.0896 (7)	3.6 (4)
C5C	−0.2092 (5)	0.3528 (6)	0.1155 (7)	3.3 (4)
C6C	−0.1563 (5)	0.3513 (6)	0.1295 (6)	3.3 (4)
C1D	−0.0678 (5)	0.3729 (6)	0.0841 (6)	2.6 (4)
C2D	−0.0376 (5)	0.4323 (7)	0.1174 (4)	3.2 (4)
C3D	−0.0398 (5)	0.4905 (6)	0.0776 (6)	3.3 (4)
C4D	−0.0722 (5)	0.4893 (6)	0.0046 (6)	3.4 (4)
C5D	−0.1024 (5)	0.4300 (7)	−0.0286 (4)	2.9 (4)
C6D	−0.1003 (5)	0.3718 (6)	0.0111 (6)	3.2 (4)
C1E	−0.1924 (5)	0.0529 (6)	0.1865 (6)	2.4 (4)
C2E	−0.1651 (4)	−0.0092 (7)	0.2166 (5)	2.7 (4)
C3E	−0.1887 (5)	−0.0733 (6)	0.1873 (6)	2.9 (4)
C4E	−0.2395 (5)	−0.0754 (6)	0.1278 (7)	4.1 (5)
C5E	−0.2668 (4)	−0.0133 (8)	0.0976 (5)	4.5 (5)
C6E	−0.2432 (4)	0.0508 (6)	0.1270 (6)	2.4 (4)
C1F	−0.0928 (4)	0.3270 (8)	0.4081 (4)	2.3 (4)
C2F	−0.0374 (4)	0.3323 (8)	0.4513 (6)	2.3 (4)
C3F	−0.0150 (3)	0.3310 (8)	0.5243 (6)	3.5 (5)
C4F	−0.0479 (5)	0.3244 (9)	0.5539 (5)	3.8 (5)
C5F	−0.1033 (5)	0.3191 (9)	0.5106 (7)	4.9 (6)
C6F	−0.1257 (3)	0.3204 (9)	0.4377 (6)	3.5 (5)
C1G	−0.1450 (5)	0.4007 (6)	0.2989 (6)	1.7 (3)
C2G	−0.2002 (4)	0.4118 (6)	0.2666 (6)	2.7 (4)
C3G	−0.2209 (4)	0.4790 (7)	0.2463 (6)	3.5 (4)
C4G	−0.1864 (5)	0.5352 (6)	0.2583 (7)	3.7 (5)
C5G	−0.1313 (5)	0.5241 (6)	0.2906 (7)	4.2 (5)
C6G	−0.1106 (3)	0.4569 (8)	0.3109 (7)	4.3 (5)

partment of the electrochemical cell was separated from the reference compartment by a modified Luggin capillary. All three compartments contained a 0.1 M solution of the supporting electrolyte.

The dichloromethane was distilled from P_2O_5 under dinitrogen prior to use. Supporting electrolyte tetrabutylammonium perchlorate (TBAP) (Southwestern Analytical Chemicals, Inc.) was used without further purification. Electrolyte solutions of methylene chloride were prepared and stored over 80–200-mesh activated alumina and activated 4-Å molecular sieves (Fisher Scientific Co.) prior to use in the experiments. In all cases working solutions were prepared by recording background cyclic voltammograms of the electrolyte solution before addition of the complex. The working compartment of the cell was bubbled with solvent-saturated argon to deaerate the solution.

Potentials are reported vs aqueous AgCl/Ag and are not corrected for the junction potential. The standard current convention is used (anodic currents are negative). To allow future corrections and the correlation of these data with those of other researchers, we have measured the $E°$ for the ferrocenium/ferrocene couple[23] under conditions identical to those used for the compounds under study. In CH_2Cl_2/TBAP, $E° = +0.505$ V. No IR compensation was used.[24]

Table III. Selected Bond Distances (Å) and Angles (deg)[a] for $[Rh_2(HTP5)_2(dppm)_2]^{2+}$ Cation

Distances			
Rh1–Rh2	3.070 (3)	Rh2–C7	1.96 (2)
Rh1–C1	1.95 (2)	Rh2–P2	2.279 (4)
Rh1–P1	2.320 (5)	C7–N7	1.15 (3)
C1–N1	1.15 (3)	N7–C6	1.45 (3)
N1–C2	1.49 (3)	P2–C1P	1.79 (2)
P1–C1P	1.86 (2)		
Angles			
P1–Rh1–P1	179.7 (3)	P2–Rh2–C7	87.7 (5)
P1–Rh1–C1	88.3 (6)	P2–Rh2–C7	92.5 (5)
P1–Rh1–C1	91.7 (6)	C7–Rh2–C7	169 (1)
C1–Rh1–C1	174 (1)	Rh2–C7–N7	177 (2)
Rh1–C1–N1	177 (2)	C7–N7–C6	172 (1)
C1–N1–C2	179 (2)	Rh2–P2–C1P	110.3 (5)
Rh1–P1–C1P	113.0 (7)	Rh2–P2–C1C	119.0 (5)
Rh1–P1–C1A	120.0 (6)	Rh2–P2–C1D	113.9 (4)
Rh1–P1–C1B	118.4 (4)	P1–Rh1–Rh2–P2	23.8
P2–Rh2–P2	177.9 (3)	C1–Rh1–Rh2–C7	27.8

[a] Estimated standard deviation in parentheses.

Spectroelectrochemical Experiments. Infrared and UV–vis spectral changes during thin-layer bulk electrolyses were observed using a flow-through spectroelectrochemical thin-layer cell as described previously.[25] Infrared data were collected on a Mattson Sirius 100 spectrometer. All IR data were corrected for a stray light error (13%) that originates from the inadvertant collection of light reflected off the front face of the CaF_2 plate of the spectroelectrochemical cell. Bulk electrolyses in the IR thin cell were controlled by an Electrosynthesis Co. (ESC) 410 potentiostatic controller and an ESC 420-A accessory power unit.

UV–vis spectra were recorded on a Tracor Northern TN-6500 rapid-scan diode-array apparatus. The light source was a Xe arc lamp. Bulk electrolyses in the UV–vis thin cell were controlled by the BAS-100 thin-layer bulk electrolysis program.

Results

Characterization and Structural Analysis. The blue product $[Rh_2(HTP5)_2(dppm)_2](PF_6)_2$ is formed at room temperature by the rapid reaction of $[Rh(dppm)(CO)Cl]_2$ with the HTP5 ligand followed by the addition of NH_4PF_6. Infrared spectra of the reaction mixture, prior to the addition of NH_4PF_6, identify the head-to-head binuclear compound as the major isocyanide-containing product (vide infra). The binuclear nature of the complex was verified by FABMS and X-ray crystallography.

The structure of $[Rh_2(HTP5)_2(dppm)_2](PF_6)_2$, Figure 1, is composed of bridged, binuclear cations with distorted square-planar arrangements of ligands around each of the Rh(I) metal centers. As with the other binuclear $Rh_2(dppm)_2L_4$ compounds, the two diisocyanide and diphosphine ligands are mutually trans.[3,26,27] The most interesting feature of the structure is that the diisocyanide ligands are attached in the head-to-head configuration. The Rh–Rh distance of 3.070 (3) Å is slightly shorter than typical distances for Rh(I) binuclear complexes that contain the dppm bridging ligand.[3,28] As with other "face-to-face" compounds of similar structure, the two metal centers adopt square-planar geometries in which the metal–ligand planes are perpendicular to the metal–metal axis. The CN groups are bent out of this plane (C1–Rh1–C1 and C7–Rh2–C7 bond angles are 174 (1) and 169 (1)°, respectively) and toward the phosphorus atoms (P–Rh–C bond angles are approximately 88°), resulting

(23) Koepp, H. M.; Wendt, H.; Strehlow, H. *Z. Z. Elektrochem.* **1960**, *64*, 483.
(24) Gagne, R. R.; Koval, C. A.; Lisensky, G. C. *Inorg. Chem.* **1980**, *19*, 2854.
(25) Bullock, J. P.; Mann, K. R. *Inorg. Chem.* **1989**, *28*, 4006.
(26) (a) Mague, J. T.; DeVries, S. H. *Inorg. Chem.* **1980**, *19* (12), 3743. (b) Mague, J. T.; Sanger, A. R. *Inorg. Chem.* **1979**, *18* (8), 2060. (c) Verkade, J. G. *Coord. Chem. Rev.* **1972**, *9*, 1.
(27) Balch, A. L. *J. Am. Chem. Soc.* **1976**, *98*, 8049.
(28) Cowie, M.; Dwight, S. K. *Inorg. Chem.* **1980**, *19*, 2500.

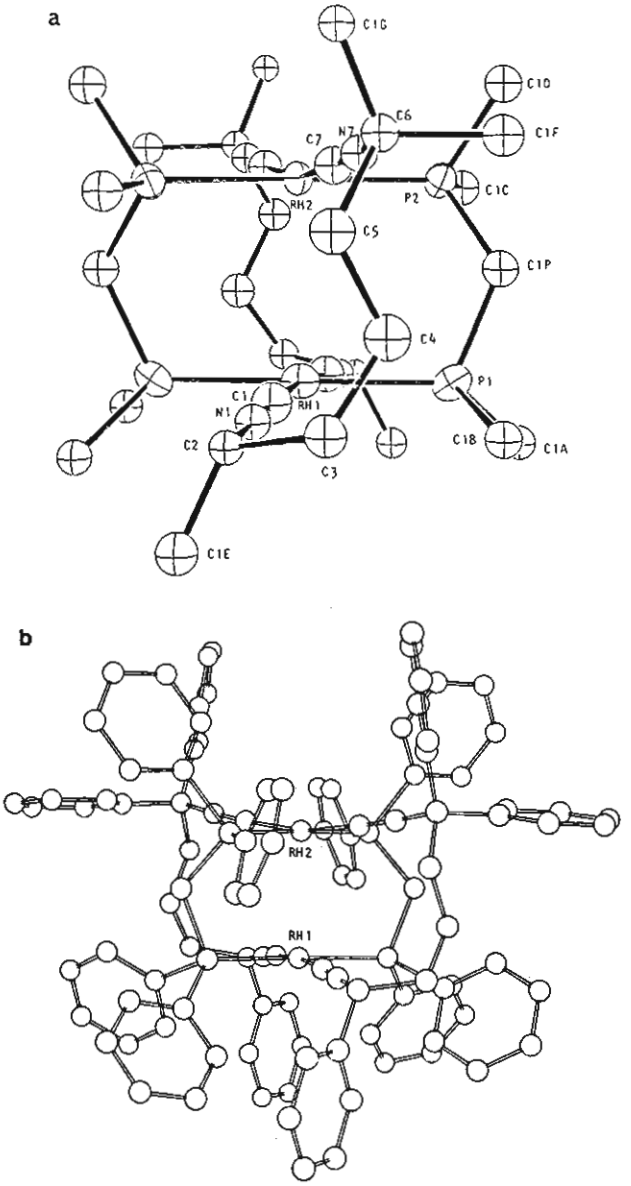

Figure 1. (a) ORTEP drawing of $[Rh_2(HTP5)_2(dppm)_2]^{2+}$ cation showing the atomic numbering scheme (only the first carbon of the phenyl rings are shown for clarity). (b) PLUTO drawing of $[Rh_2(HTP5)_2(dppm)_2]^{2+}$ cation. RH1 indicates the tail end of the molecule.

in a slight deviation from idealized square-planar geometry. The Rh–C and Rh–P distances and P–Rh–P angles given in Table III are typical. Of interest is the nonequivalence of the two Rh–P distances. The Rh1–P distance of 2.320 (5) Å is significantly longer (8σ) than the Rh2–P distance 2.279 (4) Å. We believe these bond length differences are induced by the severe steric interactions at the "head" end of the molecule.

Instead of the usual eclipsed conformation, the Rh square-planar units are twisted relative to each other at an angle of 26°. As a result of this twist, all six phenyl rings at the "tail" end of the molecule (the Rh1 end) are approximately equidistant from the center of the molecule. At the head end, however, four of the eight phenyl rings are in the C–Rh–P plane while the other four are positioned further along the metal–metal axis from the center of the molecule, Figure 1b. Examination of the four phenyl rings in the C–Rh–P plane shows that the two rings which are attached to the isocyanide ligand (F rings) are nearly coplanar with the C–Rh–P plane while the two rings on the dppm ligand (C rings) are perpendicular to it.

Finally, while the HTP5 ligand exists as a 1:1 mixture of *R* and *S* optical isomers, the structure of the dication indicates unambiguously that the two HTP5 ligands within a given molecule are the same optical isomer.[29] This result is somewhat surprising

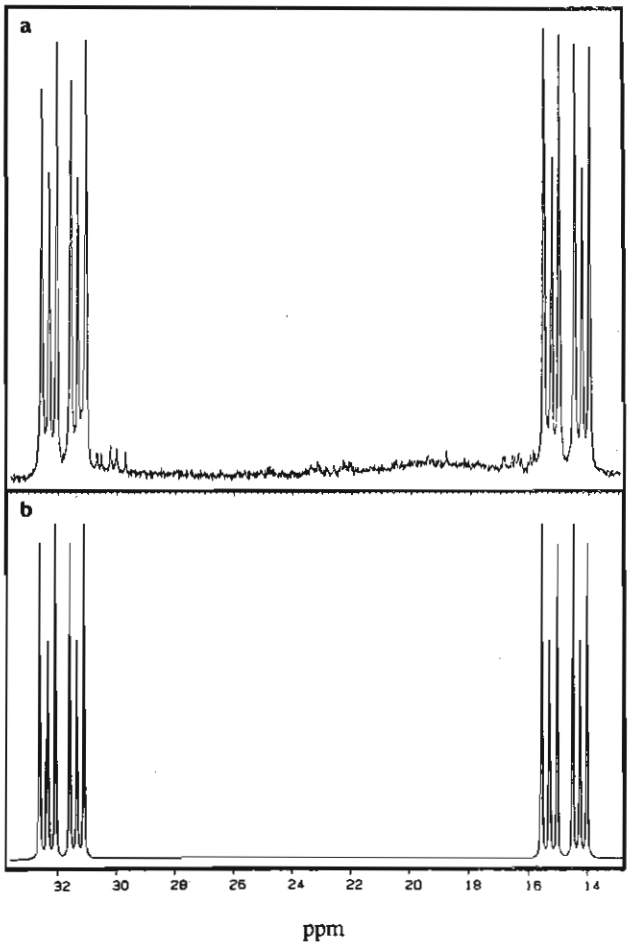

Figure 2. (a) $^{31}P\{^1H\}$ NMR spectrum of $[Rh_2(HTP5)_2(dppm)_2](PF_6)_2$ in deuteriodichloromethane. (b) Simulated $^{31}P\{^1H\}$ NMR spectrum.

and will be discussed below.

^{31}P and Homonuclear 2D δ/J Resolved ^{31}P NMR. The ^{31}P NMR spectrum of $[Rh_2(HTP5)_2(dppm)_2](PF_6)_2$ in dichloromethane at room temperature reveals two nonoverlapping doublets of "triplets",[30] one centered at 31.59 ppm and the other at 14.74 ppm, Figure 2. The septet due to the PF_6^- anion is centered at −143.93 ppm. By comparison, the ^{31}P NMR of $[Rh_2(dimen)_2(dppm)_2](PF_6)_2$, Figure 3, shows three nonoverlapping doublets of triplets. The two outer sets of peaks (HH and HH′) have a pattern similar to that of $[Rh_2(HTP5)_2(dppm)_2](PF_6)_2$. The inner doublet of triplets (HT) has a 1:2:1:1:2:1 pattern.

The homonuclear 2D δ/J resolved ^{31}P NMR spectra of $[Rh_2(HTP5)_2(dppm)_2](PF_6)_2$ and $[Rh_2(dimen)_2(dppm)_2](PF_6)_2$ were obtained to clarify the assignment of chemical shifts and couplings. After tilting, the f_2 axis only contains information about the phosphorus chemical shifts and P–Rh coupling. Along this axis, the ^{31}P spectrum of $[Rh_2(HTP5)_2(dppm)_2](PF_6)_2$ collapses into two doublets at 31.73 and 14.75 ppm with respective values for J_{P-Rh} of 120.85 and 124.53 Hz. The view along the f_1 axis (which yields P–P coupling information) shows triplets for each of the four peaks observed along the f_2 axis. The splitting between the two outer peaks of each triplet gives a P–P coupling of 62.25 Hz. In the ^{31}P 2D δ/J experiment, the spectrum of $[Rh_2(dimen)_2(dppm)_2](PF_6)_2$ collapses to three doublets, δ = 26.39, 23.83, and 21.17 ppm (respective J_{P-Rh} = 121.5, 125.5, and 125.2 Hz) on the f_2 axis. The f_1 axis shows triplets for each of the six peaks on the f_2 axis.

(29) Disordering of the *R* and *S* isomers can be ruled out because it would involve switching a H atom for a phenyl ring. The X-ray data, although not of the highest quality, unambiguously rule out this possibility.

(30) We refer to the three-line pattern produced by the second-order nature of these spectra as a triplet although they do not follow the binomial (1:2:1) intensity pattern.

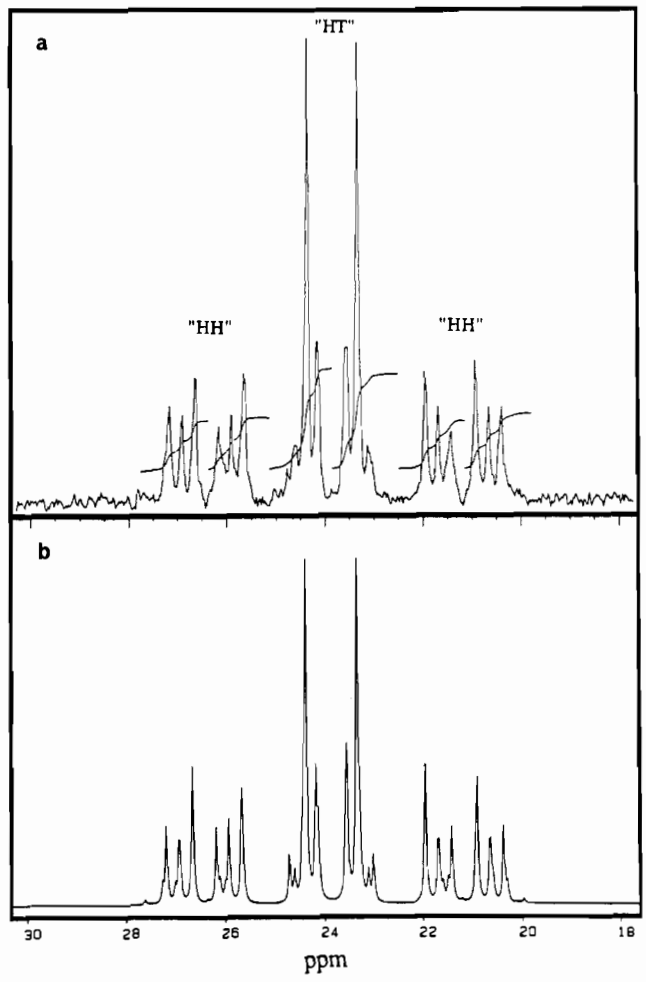

Figure 3. (a) $^{31}P\{^1H\}$ NMR spectrum of $[Rh_2(dimen)_2(dppm)_2](PF_6)_2$, in deuterioacetone. (b) Simulated $^{31}P\{^1H\}$ NMR of spectrum. Peaks due to the head-to-head isomer are indicated by HH while those due to the head-to-tail isomer are labeled with HT.

Infrared and UV–Vis Spectra. The infrared spectrum of $[Rh_2(HTP5)_2(dppm)_2](PF_6)_2$ obtained in CH_2Cl_2 contains two bands in the C≡N stretching region at 2144 and 2110 cm^{-1}. The spectrum obtained in a Nujol mull is identical except that the band at 2110 cm^{-1} is shifted to 2104 cm^{-1}.

The UV–vis absorption spectra of room temperature solutions of $[Rh_2(HTP5)_2(dppm)_2]^{2+}$ exhibit the characteristic,[3,31-33] low-energy $^1A \rightarrow {}^1B_1$ ($d_{\sigma^*} \rightarrow p_\sigma$) absorption band at 591 nm (ϵ = 8630 M^{-1} cm^{-1}). Room temperature solutions also exhibit a strong emission band at 676 nm which we assign as fluorescence from the $^1B_1[^1(d_{\sigma^*}p_\sigma)]$ state.

Electrochemical and Spectroelectrochemical Studies. The cyclic voltammogram of $[Rh_2(HTP5)_2(dppm)_2](PF_6)_2$ in CH_2Cl_2/TBAP shows a quasi-reversible oxidation with $E^{\circ\prime}$ = 702 mV that we assign to the 3+/2+ couple. Double-potential step chronocoulometry experiments over the 3+/2+ couple and thin-layer bulk electrolysis confirm this to be a quasi-reversible one-electron oxidation.[34] Also present is an irreversible 3+ to 4+ oxidation $E_{p,a}$ = 1407 mV. Large-scale electrolysis (1 h) designed to produce the d^7–d^8 radical at ambient temperatures failed, but thin-layer spectroelectrochemical oxidations designed to produce the radical on a faster time scale (2 min) were successful (vide infra).

The infrared spectral changes for the one-electron oxidation of $[Rh_2(HTP5)_2(dppm)_2](PF_6)_2$ in CH_2Cl_2/TBAP are shown in Figure 4. The process proceeds cleanly as indicated by the isosbestic point. Both ν(CN) stretching frequencies increase in energy, by 39 cm^{-1} upon oxidation by one electron, from 2143 and 2111 cm^{-1} to 2182 and 2149 cm^{-1}, respectively. The relatively high values for the ν(CN) stretches observed for the radical are consistent with a substantial decrease in electron density at the Rh–Rh core.

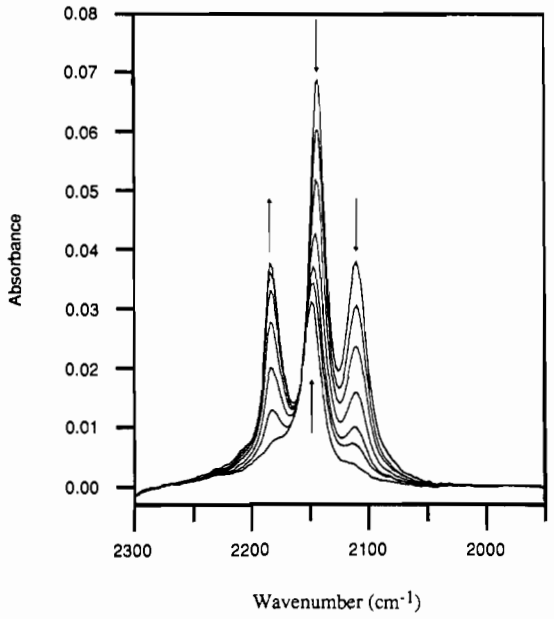

Figure 4. Infrared spectral changes that result during the electrolysis of a 1.0 mM solution of $[Rh_2(HTP5)_2(dppm)_2](PF_6)_2$ in CH_2Cl_2/TBAP.

Table IV. Possible Isomeric Arrangements for $[Rh_2(HTP5)_2(dppm)_2](PF_6)_2$

ligand arrangement	chirality of HTP5 ligands		
	first HTP5	second HTP5	
head-to-head	*R*	*R*	enantiomers
	S	*S*	
	R	*S*	identical
	S	*R*	
head-to-tail	*R*	*R*	enantiomers
	S	*S*	
	R	*S*	identical
	S	*R*	

The UV–vis spectral changes for the one-electron oxidation in CH_2Cl_2/TBAP are shown in Figure 5. The process proceeds cleanly as indicated by the isosbestic point. The absorbances at 591 and 322 nm due to the Rh(I)Rh(I) compound decrease in intensity as the peaks due to the radical grow into the spectrum at 605 and 450 nm. Consistent with previous reports[3] we tentatively assign the intense, higher energy feature to the $d_\sigma \rightarrow d_{\sigma^*}$ transition and the weaker, lower energy transition to a $d_{\sigma^*} \rightarrow p_\sigma$ one-electron excitation.

EPR Spectra. A solution of the $[Rh_2(HTP5)_2(dppm)_2]^{3+}$ radical was prepared by adding 1 equiv of $AgPF_6$ dissolved in CH_2Cl_2 (5.3 mL, 0.010 mmol) to a 1.0 mM solution of $[Rh_2(HTP5)_2(dppm)_2](PF_6)_2$ (10 mL, 0.010 mmol) in CH_2Cl_2/TBAP. The resulting green solution was immediately frozen. Three signals are observed in the frozen solution spectrum at 100 K. Solutions at ambient temperatures turn blue within minutes, probably due to a disproportionation reaction that regenerates the $[Rh_2(HTP5)_2(dppm)_2]^{2+}$ complex. The EPR spectrum is included as supplementary material.

Discussion

Characterization and Structural Analysis. There are eight possible configurations of the $[Rh_2(HTP5)_2(dppm)_2]^{2+}$ complex which result from various combinations of the two optical isomers of the HTP5 ligand and the two possible arrangements of the two ligands (head-to-head and head-to-tail). As indicated in Table

(31) Miskowski, V. M.; Nobinger, G. L.; Klinger, D. S.; Hammond, G. S.; Lewis, N. S.; Mann, K. R.; Gray, H. B. *J. Am. Chem. Soc.* **1978**, *100*, 485.
(32) Fordyce, W. A.; Crosby, G. A. *J. Am. Chem. Soc.* **1982**, *104*, 985.
(33) Che, C. M.; Lee, W. M. *Chem. Commun.* **1986**, 616.
(34) $E^{\circ\prime}_{3/2}$ = +702 mV, ΔE_p = 113 mV, $i_{p,c}/i_{p,a}$ = 0.93, D = 4.7 × 10^{-6} cm^2/s.

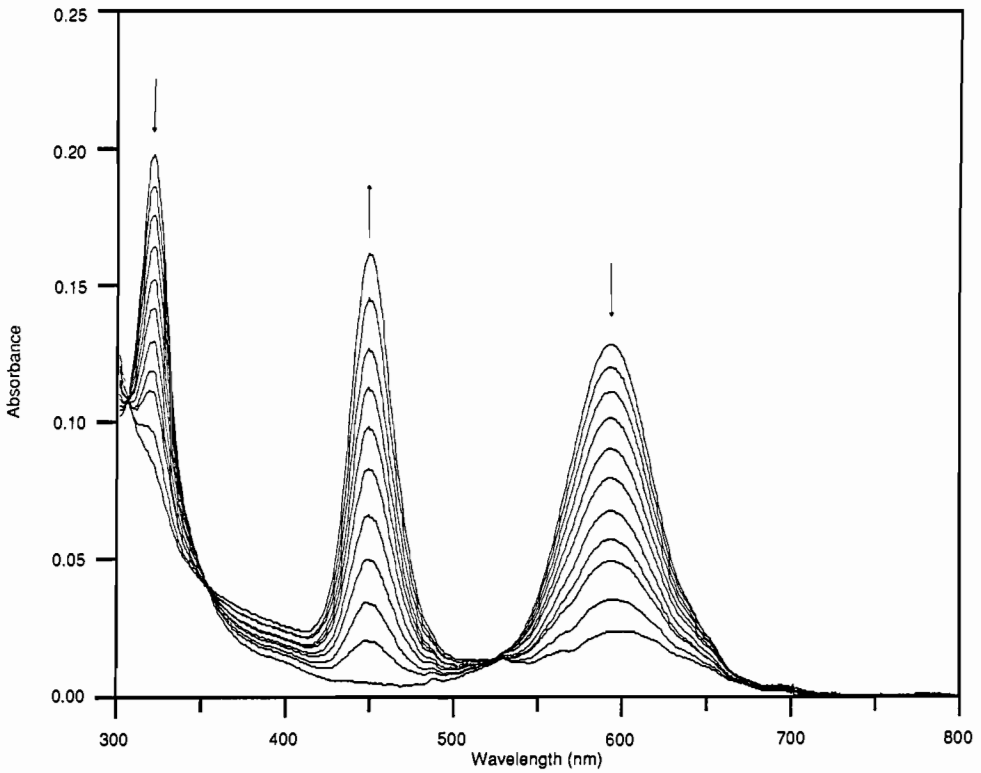

Figure 5. UV–vis spectral changes that result during the electrolysis of a 1.0 mM solution of $[Rh_2(HTP5)_2(dppm)_2](PF_6)_2$ in CH_2Cl_2/TBAP.

IV, two pairs are enantiomers and two pairs are identical, leaving six different possible isomers. Our "chemical intuition" initially suggested to us that the head-to-tail configurations with seven phenyl groups at each end would be more stable than the head-to-head isomers, but the structure of the selected crystal shows only the head-to-head *SS* and *RR* isomers to be present. This solid-state structure is representative of the bulk sample and solutions as confirmed by infrared and ^{31}P NMR data (vide infra).

To test possible reasons why our chemical intuition failed to predict the correct isomer of the compound, the MMX energies of the six different isomers were calculated using the molecular modeling program PCMODEL.[35] The calculations determined that all three head-to-head isomers have equal energies. The three head-to-tail isomers also have equal energies but are higher than the head-to-head isomers by 7 kcal/mol. Thus, MMX energies are consistent with the formation of head-to-head isomers. Entropic effects and distortions in the Rh square-planar unit which are ignored in the MMX calculations could result in a lower energy for the observed head-to-head *RR* and *SS* enantiomeric isomers than that for the unobserved head-to-head *RS*/*SR* isomer. These calculations were also performed for the molecular analogs in which all phenyl groups were replaced by methyls. In these methylated compounds *all* isomers are equivalent in energy, indicating that enthalpic steric interactions among the phenyl groups play the major role in determining the energy differences among the $[Rh_2(HTP5)_2(dppm)_2](PF_6)_2$ isomers.

The head-to-head arrangement places six phenyl groups in the region of one Rh (tail) and eight phenyl rings around the other (head), resulting in one sterically crowded end (eight phenyls) and one less crowded end (six phenyls). This ligand arrangement produces a C_2 axis along the Rh–Rh bond instead of perpendicular to it as would be in the case of the head-to-tail isomer.

This ligand conformation also points the hydrogen on the C2 carbon directly at the phenyl ring of the dppm which bisects the C–Rh–P plane at the head end. Replacing this hydrogen with a phenyl would cause the two rings to collide. This result seems to rationalize our inability to synthesize $[Rh_2(TP5)_2(dppm)_2](PF_6)_2$ and the head-to-tail isomers of $[Rh_2(HTP5)_2(dppm)_2](PF_6)_2$. This phenyl ring from the dppm also appears to prevent the carbon backbone of the HTP5 ligand from twisting in the direction necessary for the head-to-head *RS* isomer to form.

To accommodate the eight phenyl rings at the head of the molecule, four rings (C and F) are placed in the C7–Rh2–P2 plane while four others are placed in the perpendicular plane further from the center of the molecule. These steric interactions twist the dppm ligands to an angle of 26° between the two Rh square-planar units. This twist also results in a slightly shorter Rh–Rh distance (3.070 (3) Å) than is typical for Rh(I) binuclear complexes that contain the dppm bridging ligand.[3,28] For example, a Rh–Rh distance of 3.161 (1) Å is reported for the eclipsed conformation $[Rh_2(dimen)_2(dppm)_2](PF_6)_2$.[3] The twist also distorts the carbon backbone of the HTP5 ligand into the anti–gauche conformation which is only slightly higher in energy than the preferred anti–anti conformation. The most interesting result of the 26° twist is the difference in the rotameric conformations about the Rh1–P1 and Rh2–P2 bonds. At the Rh2 end, the α-phenyl ring carbon (C1C) is in the $Rh2(P2)_2(C7)_2$ square plane. At the Rh1 end, the methylene carbon (C1P) is aligned nearly parallel with the Rh1–Rh2 vector. These conformational effects are expected to produce significant differences in the Rh–P π interactions at the two ends. These π bonding differences are observable in the Rh1–P1 and Rh2–P2 bond distances, the ^{31}P chemical shift, and the ν(CN) stretching frequency and intensity observed for the Rh1 and Rh2 centers (vide infra).

^{31}P and Homonuclear 2D δ/J Resolved ^{31}P NMR. The AA′MM′XY pattern of the ^{31}P NMR spectrum of $[Rh_2(HTP5)_2(dppm)_2](PF_6)_2$ is consistent with the solid-state structure, indicating that it is retained in solution and the bulk sample consists of the same two isomers as the crystal used in the X-ray structural analysis. We addressed the possibility that crystals containing other isomers might exist in the bulk material. Although the *RR* and *SS* head-to-head isomers would be chemically equivalent, the other isomers would not and their ^{31}P NMR spectra should be different. There is no spectral evidence to support the existence of these isomers in solutions.

(35) Serena Software, Bloomington, IN; 1990. PCMODEL Version 4.0 was written for IBM AT compatible microcomputers and uses MMX calculations developed by J. J. Gajewski and K. E. Gilbert. For minimizations, the Rh atoms were set to square-planar geometry with neutral charge. The axial positions were filled by placing a bond between the metals and lone pair electrons at the external axial site of each metal. The Rh–Rh distance was fixed at 3.07 Å.

Table V. $^{31}P\{^1H\}$ NMR Spectroscopic Data for $[Rh_2(LL)_2(dppm)_2](PF_6)_2$

	^{31}P chemical shift (δ (ppm)	coupling constant J (Hz)	
	$[Rh_2(HTP5)_2(dppm)_2](PF_6)_2$ in CH_2Cl_2		
	31.73	P–Rh	120.85
		P_{trans}–P	350
		P–P	62.25
	14.75	P–Rh	124.53
		P_{trans}–P	350
		P–P	62.25
	$[Rh_2(dimen)_2(dppm)_2](PF_6)_2$ in Acetone		
HH	26.39	P–Rh	121.51
		P_{trans}–P	350
		P–P	63.93
HH	21.17	P–Rh	125.17
		P_{trans}–P	350
		P–P	63.93
HT	23.83	P–Rh	125.5
		P_{trans}–P	350
		P–P	65

To clarify the assignment of chemical shifts and couplings in the ^{31}P NMR spectra of $[Rh_2(HTP5)_2(dppm)_2](PF_6)_2$, the homonuclear 2D δ/J resolved ^{31}P NMR spectrum was obtained. Along the f_2 axis, the ^{31}P spectrum collapses into two doublets at 31.73 and 14.75 ppm with respective values for J_{P-Rh} of 120.85 and 124.53 Hz. These J_{P-Rh} values are typical for rhodium(I) phosphine compounds.[26] This experiment indicates that there are two types of phosphorus atoms with surprisingly different chemical shifts. The view along the f_1 axis (which yields P–P coupling information) shows triplets for each of the four peaks observed along the f_2 axis. The separation of 62 Hz between the outer peaks of each triplet is typical for the coupling between phosphorus atoms within a given dppm.[26] From NMR simulations (Table V, Figure 2B) we also determined that the center peak of each triplet results from strong coupling ($J > 300$ Hz) between phosphorus atoms with the same chemical shift. This coupling is in the range previously reported for trans P–Rh–P coupling constants (300–450 Hz).[26]

The cause of the 17 ppm difference in the chemical shifts observed for the head and tail ends of the molecule is of interest. We suggest that it is due to different π bonding components in the Rh–P interactions at the two ends induced by the previously described rotameric conformations of the substituents around the Rh–P bonds. To further support this idea, we decided to reinvestigate the ^{31}P NMR spectra of $[Rh_2(dimen)_2(dppm)_2]^{2+}$ which has coordination geometries, including the rotameric conformation, at both Rh atoms that are nearly identical.[3] The ^{31}P NMR spectrum of $[Rh_2(dimen)_2(dppm)_2](PF_6)_2$, Figure 3a, contains a AA′MM′XY pattern (outer lines) similar to that of $[Rh_2(HTP5)_2(dppm)_2](PF_6)_2$ plus a AA′A″A‴XX′ pattern centered between the AA′MM′XY pattern. Only two isomers of the $[Rh_2(dimen)_2(dppm)_2](PF_6)_2$ compound are possible due to the achiral nature of the dimen ligand. The head-to-head isomer of the dimen complex is expected to produce a ^{31}P NMR pattern similar to that of $[Rh_2(HTP5)_2(dppm)_2](PF_6)_2$. In the head-to-tail isomer, the Rh's are related by a C_2 axis and all of the phosphorus atoms are related by combinations of the C_2 axis and a mirror plane perpendicular to this axis. The inner doublet of triplets (HT) has a AA′A″A‴XX′ pattern similar to those of $[Rh_2(LL)_2(dppm)_2](PF_6)_2$, where LL = bridge (1,3-diisocyanopropane),[36] and $[Rh(t\text{-}C_4H_9NC)_4(dppm)_2](PF_6)_2$.[26a] In these latter cases only a single isomer is possible. By analogy to $[Rh_2(HTP5)_2(dppm)_2](PF_6)_2$ the outer peaks of the ^{31}P NMR (HH) are assigned to the head-to-head isomer while the inner peaks (HT) are assigned to the head-to-tail isomer. Further evidence of this assignment comes from the ^{31}P 2D δ/J NMR spectrum of $[Rh_2(dimen)_2(dppm)_2](PF_6)_2$. In this case the f_2 axis displays three doublets, δ = 26.39, 23.83, and 21.17 ppm (J_{P-Rh} = 121.5, 125.5, and 125.2 Hz, respectively), where the intensity of the peaks at 23.83 ppm is twice that of the other peaks. The presence of three different phosphorus chemical shifts indicate that two isomers exist.

Integration of the ^{31}P NMR spectra shows the combined area of the two sets of outer peaks (HH) to be equal to the area of the inner peaks (HT). Thus, equal amounts of the head-to-head and head-to-tail isomers are present as is expected from purely statistical calculations. As shown in previous work,[8,9] the lack of selectivity in the dimen ligand binding arrangement also indicates that only a slight steric and electronic difference exists between the two ends of the dimen ligand. The chemical shifts of the phosphorus atoms in the head-to-head isomers of $[Rh_2(dimen)_2(dppm)_2](PF_6)_2$ and $[Rh_2(HTP5)_2(dppm)_2](PF_6)_2$ in acetone solutions support this conclusion. In the compound containing dimen the difference is only 5.22 ppm while for the compound containing HTP5 the difference is 16.98 ppm.

Infrared Spectra. The IR spectrum of $[Rh_2(HTP5)_2(dppm)_2](PF_6)_2$ exhibits two peaks (2144 and 2110 cm^{-1}) both in Nujol mulls and in solutions. Furthermore, the relative intensity ratios are nearly identical (1.9:1 and 2.1:1, respectively). This result suggests that the solid-state structure, including the twist, persists in solution.

Four isocyanide stretching frequencies, two with A symmetry and two with B symmetry, are predicted for $[Rh_2(HTP5)_2(dppm)_2](PF_6)_2$ with C_2 symmetry. However, only the z component (colinear with the Rh–Rh bond) of the net transition moment vectors of the frequencies with A symmetry contribute to the A mode intensities. Hence, these intensities are highly dependent on the extent to which the isocyanide triple bonds are bent out of the plane of the metal centers. In the nearly idealized geometry with planar $Rh(CN)_2P_2$ units exhibited by $[Rh_2(HTP5)_2(dppm)_2](PF_6)_2$, these vibrations would be expected to have nearly zero intensity. Thus, the strong bands at 2144 and 2110 cm^{-1} are assigned to the CN stretches with B symmetry.

Two interpretations of our observation of two strong IR bands for $[Rh_2(HTP5)_2(dppm)_2]^{2+}$ are possible. First, a vector analysis[37] of the intensities of the two bands (with the assumptions that the ν(CN) dipole vectors on different metals are coupled and each dipole has the same magnitude) yields eq 1 for the ratio of the

$$R = B_a/B_b = \cot^2 \theta \qquad (1)$$

two allowed bands with an angle of 2θ between them. Because those modes with B symmetry do not contain any component along the z axis, the angle between the net dipole vectors, 2θ, is the same as the dihedral angle between the Rh–CN bonds of the two Rh planes. When $2\theta = 0°$ (the eclipsed conformation), the intensity of B_b is zero. Application of eq 1 with the twist angle of 28° observed in the solid state predicts a ratio of 16:1. This ratio is far different from the nominal ratio of 2 we observe for solid and solution spectra. Even taking into account intrinsic differences in intensity (vide infra), this model cannot account for the discrepancy. The poor agreement suggests that a second interpretation of the two bands is more plausible. We assume that the ν(CN) dipole vector coupling is essentially zero across the long Rh–Rh interaction and the two bands arise from the two different Rh–CN–R environments at each end. We suggest that, as in the case of the ^{31}P chemical shift differences, the $Rh1(P)_2(CN)_2$ and $Rh2(P)_2(CN)_2$ ν(CN) differences result from differences in the Rh–P π bonding produced by the rotameric conformation about the Rh–P bonds fixed by phenyl ring interactions. Thus, the two ν(CN) stretches are attributed to two uncoupled, asymmetric B symmetry vibrations at each Rh center. The frequency difference of ~34 cm^{-1} is then attributed to differences in Rh—C≡N—R π bonding at Rh1 and Rh2 caused by the sterically induced differences in Rh–P π bonding at the two Rh centers. Additional evidence for this interpretation is that the 34-cm^{-1} splitting in these

(36) Mixa, M. Ph.D. Thesis, University of Minnesota, Minneapolis, MN, 1985.

(37) Cotton, F. A.; Wilkinson, G. *Advanced Inorganic Chemistry*, 4th ed.; Wiley-Interscience: New York, 1980.

two bands is not present in the free ligand which has a single ν(CN) at 2136 cm^{-1}.

This model further predicts that the differences in intensity of the two *B* symmetry bands should reflect the changes in electron density at each Rh. In other work,[25] we have shown that the integrated intensity of ν(CN) decreases with an increase in the oxidation state of the metal. A complication arises from the intrinsic differences in the integrated intensity observed for the two expected CN stretches of the uncomplexed ligand. For example, Ugi et al.[38] have shown that although ν(CN) occurs at the same frequency for benzyl isocyanide and butyl isocyanide, their integrated intensities vary by a factor of 1.6. Thus, we are unable to assign which frequency arises from which end of the molecule.

EPR Spectra. Three signals are observed in the EPR spectrum of the d^7d^8 radical in CH_2Cl_2/TBAP. The observation of three signals (g_1, g_2, g_3) for the radical under these conditions is consistent with a metal-centered radical. The low symmetry of $[Rh_2(HTP5)_2(dppm)_2]^{3+}$ ($\sim C_2$) produces one EPR signal for each of the three molecular axes. The signals at $g_2 = 2.19$ and $g_3 = 2.23$ are assigned to the two components of the **g** tensor that lie in the plane perpendicular to the Rh–Rh vector. The assignment of the signal with $g_1 = 1.99$ to the **g** value of the metal–metal principal axis is consistent with similar EPR signals observed for other binuclear Rh(I)–Rh(II) radicals previously reported.[3,4,39] The three-line pattern due to hyperfine coupling ($A = 18.02 \times 10^{-4}$ cm^{-1}) indicates that the unpaired electron is delocalized equally over the two $I = {}^1/_2$ Rh centers on the EPR time scale.[40] Although the crystal structure and ^{31}P NMR spectra indicate that the two ends of the d^8d^8 parent dication are inequivalent, the **g** value along the Rh–Rh axis (g_1) apparently is not sensitive to these differences in the Rh atom environments of the d^7d^8 radical species.

Conclusions

The synthesis of only the head-to-head geometric isomer of $[Rh_2(HTP5)_2(dppm)_2](PF_6)_2$ while both isomers of $[Rh_2(dimen)_2(dppm)_2](PF_6)_2$ form in equal amounts illustrates how interligand steric effects control product formation. We suggest that after the first HTP5 ligand attaches to the binuclear Rh_2P_4 core the molecule twists to accommodate the phenyl rings. The resulting intermediate structure then requires that the second HTP5 have the same stereochemistry as the first as it attaches to produce the head-to-head configuration. Our failure to prepare the more sterically hindered analog $[Rh_2(TP5)_2(dppm)_2](PF_6)_2$ (where TP5 = 1,5-diisocyano-1,1,5,5-tetraphenylpentane) is consistent with this view that the arrangement of the phenyl rings controls the twist away from the eclipsed conformation and determines the stereochemistry of the attack of the second HTP5 ligand. Similar reactions with smaller ligands provide further evidence for ligand control of product formation. For example, the steric and electronic differences in the ends of the dimen ligand are much smaller, and result in statistical quantities of isomers of $[Rh_2(dimen)_2(dppm)_2](PF_6)_2$[3] and $[AgIr_2(dimen)_4](PF_6)_3$.[8] It is also quite interesting that the steric effects in $[Rh_2(HTP5)_2(dppm)_2]^{2+}$ produce differences in the rotameric conformation of phosphorus substituents to such a degree to affect differences in the electronic structure of the Rh atoms at the two ends. To further probe these steric and the accompanying electronic differences at the two ends of $[Rh_2(HTP5)_2(dppm)_2]^{2+}$, we plan to study whether these differences can direct oxidative addition reactions of unsymmetrical reagents, such as methyl iodide, with the complex.

Acknowledgment. We thank Dr. Stephen Philson for assistance with the homonuclear 2D δ/J resolved ^{31}P NMR spectra, Larry Ito for assistance with ^{31}P NMR spectra, Prof. D. J. Britton for his assistance in the X-ray structure determination, and Johnson-Matthey, Inc., for a generous loan of rhodium trichloride.

Supplementary Material Available: Tables of crystallographic data and collection parameters, atomic coordinates, bond lengths, bond angles, general temperature factors, calculated hydrogen parameters, and least-squares planes for $[Rh_2(HTP5)_2(dppm)_2](PF_6)_2$ and figures of additional crystallographic views and the EPR spectrum of the d^7d^8 radical (21 pages); a table of calculated and observed structure factors (33 pages). Ordering information is given on any current masthead page.

(38) Ugi, I.; Meyer, R. *Chem. Ber.* **1960**, *93*, 238.
(39) (a) Bear, J. L.; Zhu, T. P.; Malinski, T.; Dennis, A. M.; Kadish, K. M. *Inorg. Chem.* **1984**, *23*, 674. (b) Eastland, G. W.; Symons, M. C. R. *J. Chem. Soc., Dalton Trans.* **1984**, 2193. (c) Connelly, N. G.; Finn, C. J.; Freeman, M. J.; Orpen, A. G.; Sterling, J. *J. Chem. Soc., Chem. Commun.* **1984**, 1025. (d) Fjeldsted, D. O.; Stobart, S. R. *J. Chem. Soc., Chem. Commun.* **1985**, 908. (e) Le, J. C.; Chavan, M. Y.; Chau, L. K.; Bear, J. L.; Kadish, K. M. *J. Am. Chem. Soc.* **1985**, *107*, 7195. (f) Connelly, N. G.; Garcia, G. *J. Chem. Soc., Chem. Commun.* **1987**, 246.
(40) It is possible that the 1:2:1 triplet is due to two overlapping doublets resulting from two inequivalent Rh's, but this region of the EPR spectrum was accurately simulated using the parameters listed with the program ESRa Version 1.0, Calleo Scientific Software Publishers, 1989.